Power Conversion in A Grid-Connected Residential PV System with Energy Storage Using Fuzzy Logic Controls

Oluwasola O. Ademulegun[1], Andres F. Moreno Jaramillo[2]

[1] Centre for Sustainable Technologies, University of Ulster, Jordanstown, Co Antrim BT37 0QB, Northern Ireland, UK

[2] School of Electronics, Electrical Engineering and Computer Science, Queen's University Belfast, Co Antrim, BT9 6SB, Northern Ireland, UK

Correspondence

Oluwasola O. Ademulegun, Centre for Sustainable Technologies, University of Ulster, Jordanstown, Co Antrim BT37 0QB, Northern Ireland, UK
Email: ademulegun-o@ulster.ac.uk

Summary: Increasing implementations of renewable energy resources to migrate from fossil fuel based electric power to clean energies have been creating new technical challenges due to their integration into an existing electrical grid. In this research, a power electronic converter based on fuzzy logic controller is developed to govern the transfer and control of power in a grid-connected residential Photovoltaic (PV) system with battery storage. A bidirectional dc-dc converter is designed for power transfer between the loads and the battery. A bidirectional ac-dc converter is used as the interface between the PV array and the electricity grid. The fuzzy logic controller is designed to meet the user power requirement – with the PV array and the battery sized to meet the critical load requirement on-site. The results indicate that the fuzzy logic-based power conversion helped the system to adjust to off-grid, low-battery, full-battery, and on-grid power conditions. The main merit of the design is simplicity in being able to manage the limited supplies from the grid and the renewable PV installation using carefully sized storage that serves critical loads within specific days of power autonomy.

KEYWORDS: Battery sizing, Battery storage, Bidirectional ac-dc converter, Bidirectional dc-dc converter, Fuzzy logic control, Grid-connected residential PV

List of Symbols and Abbreviations: †, Note; PV, Photovoltaic; dc, direct current; ac, alternating current; SOC, State of Charge; STC, Standard Test Conditions; MPPT, Maximum Power Point Tracking; PLL, Phase Lock Loop; DAB, Dual Active Bridge; PI, Proportional-Integral; THD, Total Harmonic Distortions; LV, Low Voltage; HV, High Voltage.

1. INTRODUCTION

Photovoltaic (PV) systems installed at residences are one of the alternative energy sources for clean energy generation. The power produced in a PV is in the direct current (dc) form. While certain instances may call for the direct use of the PV-generated dc power, [1,2] it is often required that the dc power be converted to an alternating current (ac) power for control and integration into conventional power systems – typically, integration into an electricity grid. At times, the power from an adjoining ac grid may be required to charge local storage devices; here, the ac power needs to be converted to a dc power. The dc-ac and ac-dc power conversions call for the use of an important electronic device – the converter.

Demand-side renewable energy resources could provide access to electricity when deployed in stand-alone micro grid systems. Several millions of people still do not have access to electricity globally; [3] for example, people living in some rural areas often have uncertain access to stable power supply due to limited electricity infrastructure, causing wide adoption of polluting local generators. Distributed renewable energy resources could play a key role in increasing the access to electricity in the rural and certain urban locations of both developed and developing countries, offering major social and economic benefits to people and businesses. [3] Meanwhile, at the places where there are adequate infrastructure and stable electricity supply, a combined PV and energy storage resource could help in transitioning the grid to a low-carbon energy system. However, a grid-connected residential PV and storage system requires accurate power conversion, control, and management.

The fuzzy logic control has been employed as a maximum power point tracking tool. [4-7] A fuzzy controller was used as a tool for power management in the standalone PV power system. [5] In a residential water supply system, [8] a fuzzy logic controller has been implemented to achieve energy saving, increased reliability, cost effectiveness, and improved system efficiency. The State of Charge (SOC) of a battery could be controlled with fuzzy logic controller – the control may be required to ensure that the battery do not discharge below the level that would affect its lifespan. [9,10] Zenned et al., presented a work, [11] where fuzzy logic controller in a hybrid power system was designed with respect to a typical household energy requirement – achieving more renewable energy utilization, cost saving and energy efficiency. An if-then fuzzy logic algorithm has been developed to balance an external power requirement from load with a fuel-battery

hybrid generation system – achieving optimal operational efficiency of the hybrid system while maintaining the SOC of the battery at a desired level. [12]

Similarly, using a state flow toolbox and advanced fuzzy controller, an advanced supervisory control has been designed to manage the power flow in a cell-battery hybrid system on a distribution, achieving operation-efficiency while maintaining the SOC of the battery. [13] A fuzzy logic control has been used for energy management in a dc microgrid system – with the fuzzy logic helping to keep the SOC of the battery within a specified limit, for improved battery-cycle life. [14] The frequency control of an autonomous system has been described using a two-stage adaptive fuzzy logic controller. [15] A fuzzy logic-based controller has been developed as droop control in a wind farm, [16] maintaining a desired droop rate and providing a desired frequency support for a smart grid. Using the availability of pumping resources as key inputs to a fuzzy logic controller, the irrigation risk of a solar pumping system has been mitigated in a design that achieves safe irrigations durations in a solar-powered irrigation system. [17] Also, a fuzzy logic interface has been designed to effectively manage the charge and discharge control of multiple grid-connected electric vehicles. [18]

Many of the works in the literature are either models for stand-alone setting or assumed a continuous power supply in designing power systems employing fuzzy logic control. Some do not consider controlling and optimizing the available power supply in meeting critical energy requirements and others include polluting local generators, but instead of using the polluting generators, a carefully sized storage could be used as power backup. Moreover, as suggested by Yuan et al., the overall performance of a hybrid power system may be improved with fuzzy logic controller when the unique characteristics of the local energy requirements are taken into consideration in the design. **[19]** In this work, a fuzzy-logic-controller power management is set up in a design scenario in which power availability from the grid is limited – where suitable storage sizing for adequate power supply for certain days of power autonomy would be required. This includes the design of fuzzy-logic-controlled ac-dc and dc-dc bidirectional converters for the integration of renewable energy with the grid for an energy system that could meet critical load requirements and prioritize the use of power generation from the distributed energy resources – in this case, a residential PV array with a battery storage. Taking cognizance of the latest approach to solar microgrid designs: where the dc supply from a PV source is fed directly to power dc loads without going through

a dc-ac power conversion phase, [14, 20] the dc supply from the PV array and the converted ac supply from the ac grid are set to power dc loads through dc buses – only dc loads are included in the storage equipped system.

Section two gives a description of the elemental designs of the system. Section three presents the results from the modeling with discussions. The main conclusions of the work are given in section four.

2. ELEMENTS OF THE ENERGY SYSTEM

This research is based on a system that allows bidirectional power flow from either the grid or the home-sized PV array to a dc bus at the residence. The system includes a bidirectional ac-dc converter – to transfer power between the electricity grid and a dc bus, a boost converter – to balance the power from the PV array to the dc bus, and a bidirectional dc-dc converter – to transfer power between a storage device and the dc bus. The grid-connected PV system – having the storage device and the bidirectional converters – is depicted in Fig. 1.

2.1. PV Array and Boost Converter

2.1.1. PV Sizing for Critical Load

The critical loads to be served are specified to determine the suitable size of the PV array to be installed. The total energy required for meeting the critical loads could be of any value depending on the energy needs at the location: the hypothetical residential building used in this case has critical energy demand given in Table 1. It is assumed that the loads can either be powered by a dc supply or have adaptive chargers that are powered by the dc supply.

The total energy to be consumed by the load is estimated as:

$$Energy = Quantity \times Power \times Hour \ (Wh/day) \quad (1)$$

The performance of any PV module depends on its internal characteristics; for example, the fill factor of a practical solar cell – points to how close to the ideal is the practical cell – gives a measure of how the maximum power of the cell matches that of the ideal. The higher the fill factor of the cell, the closer to the ideal is the cell. Whereas the characteristic impedance of a solar cell gives the output resistance of the cell at maximum power point.

The fill factor, the characteristic impedance, and other parameters of the PV module used, at Standard Test Conditions (STC) – at 1000 W/m^2 and at 25^{0}C – have the values given in Table 2.

Using the PV module having the parameters given in the Table 2, the total number of modules required in the PV array is:

$$Number\ of\ modules = \frac{Total\ power\ demand}{Maximum\ power\ rating\ of\ module} \quad (2)$$

The steps could be used in estimating the size of the PV required at any location, given the critical load specifications for the location.

2.1.2. Boost Converter

The boost converter performs Maximum Power Point Tracking (MPPT) to track the operation of the PV within the region of maximum power generation. Several MPPT methods could be used; for instance, the incremental conductance method, [21] the perturb & observe algorithm, [22] or the fuzzy based MPPT method. [7]

The boost converter has the configuration depicted in Fig. 2. The selection of values for the components have been described. [23] The designs of the major components of the converter are outlined for emphasis as follows:

2.1.2.1. Duty Cycle of the Boost Converter

With respect to Fig. 2, the duty cycle of the boost converter is given as: [23]

$$D = 1 - \frac{V_{in}\eta}{V_{out}} \quad (3)$$

D is the duty cycle, V_{in} is the input voltage, V_{out} is the output voltage, $Efficiency\ (\eta)$ accounts for the energy dissipation within the boost converter, and could be taken as 95%. [23]

2.1.2.2. Selection of Inductor

A higher inductor value gives a higher maximum current in the output. The equation for the estimation of an appropriate inductor is given as: [23]

$$L = \frac{V_{in} \times (V_{out} - V_{in})}{\Delta I_L \times f_s \times V_{out}} \quad (4)$$

where L is the inductor value, V_{in} is the input voltage, V_{out} is the output voltage, f_s is the switching frequency of the converter, ΔI_L is the approximate inductor ripple current given as: [23]

$$\Delta I_L = 0.2 \times I_{out(\max)} \times \frac{V_{out}}{V_{in}} \quad (5)$$

where $I_{out(max)}$ is the maximum output current from the supply.

2.1.2.3. Selection of Capacitor

The output capacitor is chosen to effectively remove any output voltage ripples. [23,24] The equation for the estimation of an appropriate capacitor is given as: [23]

$$C_{out(min)} = \frac{I_{out(max)} \times D}{f_s \times \Delta V_{out}} \quad (6)$$

where $C_{out(min)}$is the approximate output capacitor value, $I_{out(max)}$ is the maximum output current from the supply, D is the duty cycle, f_s is the switching frequency, and Δ V_{out} is the approximate output ripple voltage given as: [23]

$$\Delta V_{out(ESR)} = ESR\ of\ C_{out(max)} \times \left(\frac{I_{out(max)}}{1-D} + \frac{\Delta I_L}{2}\right) \quad (7)$$

where ΔI_L is the approximate inductor ripple current, *ESR* is the Equivalent Series Resistance of the selected output capacitor.

2.2. DC Bus

For a grid-connected PV system, the voltage level chosen for the dc bus is dependent on two design considerations:

- ✓ The voltage level of the electricity grid
- ✓ The size of PV array

2.2.1. Voltage Level of Grid

The grid to which the dc bus is to be connected to is at 240V/50Hz. A variation in grid voltage of about $\pm 10\%$ is considerable. A $\pm 10\%$ variation of the grid voltage translates to 217V < $\mathbf{V_{rms}}$ < 265V/50Hz and a peak equivalent value of 306V < $\mathbf{V_{peak}}$ < 375V/50Hz. A 380V bus meets the voltage level requirement.

2.2.2. Size of PV Array

The bus voltage level is chosen to be just above the total output voltage level from the PV installation. For example, for the residential site in view, the modules are connected so that, the maximum output voltage expected from the 16-module PV array – when operating at STC (at irradiance level of 1000 W/m^2 and at a temperature of 25^{0}C) – is 346 V. The dc bus voltage is set at 380 V. The boost converter controls the output from the PV array so that a 380 V is supplied to the bus.

2.3. Bidirectional AC-DC Converter

For any grid-connected hybrid system having a storage, power may flow in two ways – from the grid or vice versa. The bidirectional ac-dc converter is required to allow the two-way transfer of power. It could be designed – depending on the ac power supply – as a single-phase bidirectional ac-dc converter or a three-phase bidirectional ac-dc converter. The single-phase bidirectional ac-dc converter topology including a Dual Active Bridge (DAB) structure, the converter block, and its Phase Lock Loop (PLL) block are depicted in Fig. 3, Fig. 4, and Fig. 5, respectively. The single-phase bidirectional ac-dc converters are deployed around buildings of residential sites since the buildings are usually linked to a phase of the electricity grid.

The control elements included in Fig. 4 is designed to keep the dc bus at the end of the DAB at a constant voltage level, where a reference voltage is compared to the actual voltage to generate switching pulses moderated by a Proportional-Integral (PI) controller. The DAB structure is used because it could be easily controlled with many well-known control methods and permits the use of the control techniques that include duty cycle. [25] Moreover, while the structure uses more components, the transformer included in the structure helps to isolate one part of the system from the other, improving safety.

Meanwhile, the overall "AC-to-DC" conversion process is divided into three stages: first AC-(PLL)-to-dc, followed by a dc-to-ac transformation, and ac-to-DC after transformation – using the left-to-right conversion operation as example. Whereas the PLL keeps track of the phase of the signal at the converter-grid interface. The control helps in achieving the required stability features while maintaining a constant phase between the voltage and the current within the system. A capacitor at the dc end of the converter helps to reduce the ripples in the output current and voltage. [23,24] A current controller determines the actual minimum dc link voltage required for the grid connection. The controller measures the current output of the terminal voltage and compares it with a reference current signal so that the output current is regulated to follow a reference signal.

The grid-connected bidirectional ac-dc converter is designed to prevent unacceptable Total Harmonic Distortions (THD). A filter processes out the signals with the desired frequency – signals below a cut-off frequency. This is important for maintaining a standard THD in the power supplied to the grid. The THD should be less than 5% as

stipulated in the *IEEE 1547* guideline. [26] Meanwhile, the inductor at the ac end of the converter controls the current through the converter. [23]

In supplying power from the 380V-dc bus to the grid, the bidirectional ac-dc converter acts as a constant current source, supplying a constant current to the grid.

2.4. Battery Storage and Bidirectional DC-DC Converter

2.4.1. Battery Sizing

The modular nature of batteries makes them desirable for residential storage applications. The battery size must be large enough to meet the requirements of the residence, taking into cognizance the environmental factors that could affect the availability of electricity for recharging the battery. Social and economic factors could also be considered in sizing the battery.

In the design case where the objective is to have an energy system that will maximise the use of the power generation from the PV array and allow the residence to have some days of power autonomy, the battery is sized to capture energy for local consumption.

Taking the nominal battery voltage (N_v) to be 48 V, the days of autonomy (D_a) to be three days, the battery loss factor (B_l) to be 0.85 – an 85% efficient battery – for example, a lithium ion battery – and the depth of discharge of battery (D_d) to be 0.6; the total energy demand (E_d) at the residence from Table 1 is $3.224kWh/day$, the battery capacity required (B_c) is calculated:

$$Battery\ capacity\ (B_c) \geq \frac{E_d \times D_a}{B_l \times D_d \times N_v} \tag{8}$$

$$Battery\ capacity\ (B_c) \geq 395\ Ah \cong Total\ Battery\ Ah\ required \tag{9}$$

2.4.2. Bidirectional DC-DC Converter

A means of changing voltage levels from a high voltage bus to a lower battery-charging voltage is required. The dc-dc converter transfers power between the 380V-dc bus and the low voltage (LV) dc bus. The battery and the dc loads are connected to the low voltage dc bus. Batteries are usually designed to be charged with specific voltages close to their nominal voltage. Here, the nominal charging voltage of battery storage has been set to the voltage at the lower voltage end of the dc-dc converter.

As depicted in Fig. 6, the converter used should have the bidirectional capability, having dual operating modes that allow for the exchange of power in two directions – the boost direction – where current I_1 at the low voltage side is greater than zero, and

the buck direction – where current I_1 at the low voltage side is less than zero. The basic dc-dc converters lack the ability to transfer power in two directions. This is because of the use of diodes – preventing the flow of current in the reverse direction. The combinatorial modification to the unidirectional boost and the unidirectional buck converters in achieving a bidirectional power capability of the bidirectional converter – with a description of the signal flows, operation, and control – has been described. [25,27] The basic topology of the bidirectional dc-dc converter is depicted in Fig. 7.

2.4.1.1. Duty Cycles for DC-DC Converter

The buck-boost subscripts for the elements are to reflect the mode of operation in the given converter equations: [28]

$$D_{buck} = \frac{V_{BAT}\eta}{V_{bus}} \tag{10}$$

D is the duty cycle, V_{BAT} is the battery output voltage, V_{bus} is the battery input voltage, and $Efficiency\ (\eta)$ accounts for the energy dissipation within the converter, may be taken as 95%. [23]

2.4.1.2. Inductor Selection for DC-DC Converter

The estimate for an appropriate inductor value is given as: [28]

$$L_{buck(min)} = \frac{V_{BAT} \times (V_{bus} - V_{BAT})}{0.2 \times I_{BAT} \times f_s \times V_{bus}} \tag{11}$$

while $L_{(min)}$ is the minimum inductor value for the buck or the boost mode, V_{BAT} is the battery output voltage, V_{bus} is the battery input voltage, f_s is the switching frequency, and I_{bus} is the battery input current. Meanwhile, I_{BAT} – the maximum battery current is: [28]

$$L_{boost(min)} = \frac{{V_{BAT}}^2 \times (V_{bus} - V_{BAT})}{0.2 \times I_{bus} \times f_s \times {V_{bus}}^2} \tag{12}$$

With a tolerance of 20% to compensate for aging and temperature degradations, [28]

$$L_{(min1)} = (20\% \times L_{buck(min)}) + L_{buck(min)} \tag{13a}$$

$$L_{(min2)} = (20\% \times L_{boost(min)}) + L_{boost(min)} \tag{13b}$$

2.4.1.3. Capacitor Selection for DC-DC Converter

The equations for the estimation of the approximate capacitor size are: [28]

$$C_{buck(min)} = \frac{(1 - D_{buck})}{8 \times L \times \Delta V_0 \times {f_s}^2} \tag{14a}$$

$$C_{boost(min)} = \frac{I_{BAT} \times D_{buck}}{\Delta V_0 \times V_{bus} \times f_s} \tag{14b}$$

f_s is the switching frequency, D_{buck} is the duty cycle at the buck mode, $L_{(min)}$ is the minimum inductor value, V_{bus} is the battery input voltage, and ΔV_{out} is the approximate output ripple voltage. The higher capacitor value – $C_{(min)}$ – is chosen.

As depicted in the fuzzy logic control block of Fig. 8, the two inputs of the fuzzy logic controller of the bidirectional dc-dc converter – the SOC of the battery and the voltage at the low voltage (LV) bus – are used in deciding the instantaneous direction of operation of the converter. The logic controller decides whether the converter is to operate in the buck or the boost mode.

The rule of operation for the control of the converter is defined using the fuzzy logic designer algorithm described in subsection 2.5.

2.5. Power Management System

The power management system is to permit power transfer between the grid and the dc buses. Loads are fed with the power supply from the PV array when available and from the grid or the battery when the PV supply is not available. After meeting the storage and load demands, the excess power generated from the PV array is to be sent to the grid through the 380V-dc bus.

A fuzzy logic designer is used in defining the power management rules, Table 3. The membership functions are defined to include the *SOC* of the battery, the voltage level at the LV bus – battery node denoted by *LVLoad*, and the switching direction – *Decision*; the membership functions are depicted in Fig. 9(a), 9(b), and 9(c).

The battery is to be charged or discharged following three major SOC boundaries: when the SOC of the battery is below 21%, when the SOC of the battery is between 20% and 99%, and when the SOC of the battery is above 98% – these are represented by the three membership functions *mSOC20*, *mSOC21to98*, and *mSOC100* respectively. On Fig. 9(b): when no load is connected to the LV bus, this is denoted by the *m1Vbus* membership function; when a load is powered from the LV bus, the voltage at the bus is above-zero-and-below 250 V – denoted by the *m250Vbus* membership function; when a high voltage load connects to the bus, the voltage could be above 240 V – denoted by the *mHVbus* membership function.

The triangular membership type provides suitable logical boundaries between the likely operation conditions: the type enables the decision for the charging and the discharging of the battery to be made with clear charge-discharge boundaries, and also specifies

boundaries that help to identify load and no-load bus conditions. The overlaps in the membership function happen because two membership functions could be true at some points; for example, for the SOC functions (*mSOC20* and *mSOC21to98*): this happens because the two membership functions are true at any SOC between 20% and 21%, *mSOC20* is a function that could be set true to ensure that the battery is not discharged below 20% while *mSOC21to98* is a function that could be true to permit the battery to be discharged when the SOC is above 20% – one of the membership functions ultimately wins based on the state of any other deciding functions.

When the SOC of the battery is below 21%, the bidirectional dc-dc converter is to transfer any available power at the 380V-dc bus to charge the battery. When the SOC reaches about 98%, the battery is to be kept charged while there is power supply at the 380V-dc bus. The rule specifies that the battery should be discharged only at that condition when two conditions are met: one, there is no power at the 380V-dc bus and two, when the battery SOC is above 20% – this will permit critical loads to be served from the battery when the grid and the PV array are not supplying power. Other user preferences are included in the rule set; for example, the user does not want the battery to be discharged below 20%.

The surface view for the membership functions of the fuzzy logic is depicted in Fig. 10. The result of each instantaneous computation of the algorithm determines the *Decision* switching function which in turn dictates the instantaneous operating mode of the dc-dc converter.

To verify the behaviour of the system, the possible input from practical conditions are used as test cases for performance analysis.

3. RESULTS AND DISCUSSION

The system is examined under four scenarios: First, the performance is observed when there are power inputs from both the electricity grid and the installed PV array. The second scenario is analysed using the PV array as the only power supply, this includes studying the behaviour of the system under variations in environmental conditions of temperature and irradiance. Additionally, the system is evaluated using the electrical grid as the power source; hence, no power is obtained from the PV array – typical conditions at night. The performance of the design is finally observed when there is

neither power supply from the grid nor from the PV array – when the system runs with a backup power from the battery

Meanwhile, Fig. 11 presents the summary of the designed parts of the bidirectional converter and Fig. 12(a) depicts the battery sized for meeting the critical loads on site in a use-case example of the grid-connected residential PV system. The battery is rated 48 V with 400 Ah capacity for the three days of power autonomy. To meet the same battery requirements, two numbers of 48 V 200 Ah batteries could be connected in parallel as shown in Fig. 12(b), or two numbers of four serially connected 12 V 200 Ah battery set could be connected in parallel as depicted in Fig. 12(c).

The battery recommendation for self-consumption of energy in PV applications is the deep cycle battery which permits several cycles of battery discharging. The portable, low-current charging, high efficiency, and longer-duration discharging features of the lithium ion battery make it a preferable choice to many other battery technologies. [28,29]

3.1. System with PV and Grid Power Supplies

The voltage and the current have constant phase difference, Fig. 13. This is expected to be so, the PLL has been included in the design to achieve this objective. The bidirectional ac-dc converter acts as a constant current source, supplying a constant current of about 30 A to the grid. The current level is controlled by the input inductor. For the current level depicted in Fig. 13, the inductor value is set at 50 mH.

When transferring power from the 380V-dc bus to the grid, to keep the THD in the power supplied to the grid below 5% – as discussed for a grid-connected system, with the L value of the filter being 50 mH and the C value being 0.8 mF – the THD of the system is observed at 1.93%, thus meeting the standard THD requirement.

The power supply from the PV array feeds the load and supplies the battery to full charge state. When the battery SOC is below 20.9%, the bidirectional dc-dc converter operates in the buck mode transferring power from the HV bus to the LV bus to charge the battery. The battery SOC increases as suggested from the result of Fig. 14(c). The power charges the battery until the SOC is close to 100%. Meanwhile, Fig. 14(a) and 14(b) depict the dc nature of the signal at the dc buses.

There is power supply to the battery and the dc loads at buses. For example, the power consumed by the HV-bus load is about 1.4 kW – Fig. 15(a), while the power at the LV-

bus load is about 65 W – Fig. 15(b). A net-metering device at the grid-system interface could track the net flow of current within the system.

3.2. System with Power Supply from PV Only

3.2.1. Variation in Irradiance and Temperature at Constant Load

The performance of the system is observed at irradiance level of 1000 W/m^2 and at a temperature of 25^{0}C. The irradiance level is changed to 200 W/m^2 and the temperature is adjusted to 10^{0}C to see the output of the PV array at night or near-night conditions.

The output power and the output voltage of the PV array reduces with reduced irradiance, suggesting that the system must have another power source to remain powered at the night or near-night conditions, when the irradiance level is low.

3.2.2. Variation in Load at Constant Irradiance and Temperature

The irradiance level and the temperature of the PV array are maintained at 1000 W/m^2 and 25^{0}C respectively. The load at the HV-bus is varied from 10 Ω to 100 Ω while the load at the LV-bus is varied from 5 Ω to 50 Ω. The changes in the load values mimic situations of load variations in a real system. The battery is set at a 20% initial charging state.

The system responds to the load variations while the battery is continuously charged until when it reaches full-charging state point as specified in the power management control algorithm, Fig. 16. The bidirectional dc-dc converter correctly decides that it should buck power to charge the battery – while the SOC of the battery is below 20%.

3.3. System with Power Supply from the Grid Only

The condition of having an only-grid-power-supply will subsist at nights, or during times of extreme weather, or when the PV is temporarily unavailable for maintenance. The constant power supply from the grid is fed into the system while the HV-bus load and LV-bus load are maintained at 100 Ω and 40 Ω respectively. The battery is maintained at a 20% initial charging state.

A near 1.4 kW power is observed around the load at the HV-bus, Fig. 17(a). The power around the LV-bus load is seen around 65 W, Fig. 17(b). Meanwhile, Fig. 17(c) shows the battery charging – evident from the increasing SOC.

3.4. System with No External Power Supply

Under the scenario of no external power supplies, there is neither power supply from the grid nor from the PV array. The battery has been sized to permit a continuous power supply for three days for critical loads. The critical loads specified for the residence are connected to the LV-bus. The battery capacity has been designed 48V, 400Ah. The sizing only gave consideration for backup power for critical loads at the residence for three days. The battery has not been sized to include power supply to the grid. For this test case, the battery is set to be at an initial SOC of 100% – fully charged state.

There is a power supply to the load at the LV-bus, Fig. 18(b); from a continuous battery current supply to the bus – Fig. 18(a). As depicted in Fig. 18(c), the continuous current supply leads to a continuous drop in the SOC of the battery as the logic controller prompts it to supply power to the loads at the bus, suggesting that in the absence of external power, the backup power from the battery helps to serve the critical loads.

The power supply from the battery could exceed the three days of power autonomy when the loads are served for shorter time than specified, or when less loads are served than specified in the battery sizing. However, when the loads are served for longer time than specified, or when more loads are served than specified, the power supply from the battery will usually not last for the three days. The degradation of the battery could also reduce its performance with time – this could be delayed by following the battery usage recommendations.

4. CONCLUSIONS

Fuzzy-logic-controlled converters could be used as power conversion and power management tool in a grid-connected residential PV system with storage, where the PV array and battery – used as the storage device – are sized to meet a specified on-site critical load requirements. The fuzzy logic rule has been used in modelling a renewable energy system that manages power between local energy system and the grid. The logic rules are defined such that power is derived from the PV source while the battery stores enough energy to serve the specified local loads within a given period. With the battery storage, a bidirectional dc-dc converter transfers power between the high voltage dc bus and the low voltage dc bus; a boost converter balances the power from the PV array to the high voltage end of the bidirectional dc-dc converter; and a bidirectional ac-dc converter transfers power between the grid and the rest of the system. The work serves as addition to the several use cases of fuzzy logic in the literature and is a special design case that uses fuzzy logic for converter controls: managing a grid-connected residential

PV supply and storage for autonomous supply in locations of limited or unreliable electricity supply. The residential energy systems could provide more access to clean electricity and contribute to social, economic, and environmental developments in the places of limited electricity supply.

Data Availability: The data that support the findings of this study are available on request from the corresponding author. The data are not publicly available due to privacy or ethical restrictions.

ACKNOWLEDGEMENTS

Oluwasola would like to thank the Commonwealth Commission in the UK (CSC), Swansea University, Kathryn Tomos of Swansea University, and Dr Zhongfu Zhou of Swansea University for the support of this work.

REFERENCES

1. A. Shivakumar, B. Normark, M. Welsch. Household DC networks: State of the art and future prospects. Rapid Response Energy Brief. September 2015:1-11.
2. K. Garbesi, V. Vossos, H. Shen. Catalog of DC Appliances and Power Systems. Ernest Orlando Lawrence Berkeley National Laboratory. October 2011:1-76.
3. REN21. Renewables 2019 Global Status Report (GSR 2019). Arthouros Zervos. (Paris: REN21 Secretariat). 2019; ISBN 978-3-9818911-7-1.
4. T. Bogaraj, J. Kanakaraj, J. Chelladurai. Modeling and simulation of stand-alone hybrid power system with fuzzy MPPT for remote load application. Archivals of Electrical Engineering. 2015;64(3) DOI 10.2478/aee-2015-0037: 487-504.
5. M. Venkateshkumar and Cheng Siong Chin. Fuzzy-logic Controller based Multi-port DC-DC Converter for Photo-Voltaic Power System. IOS Press eBook. 2017; DOI 10.3233/978-1-61499-927-0-663: 663-674.
6. Paramasivam Veera Manikandan, Sundaramoorthy Selvaperumal. A fuzzy-elephant herding optimization technique for maximum power point tracking in the hybrid wind-solar system. Int. Trans on Electrical Energy Systems. 2019; DOI 10.1002/2050-7038.12214.
7. Faizan Mehmood, Nouman Ashraf, Lourdes Alvarez, Tahir Nadeem Malik, Hassaan Khaliq Qureshi, Tariq Kamal. Grid integrated photovoltaic system with fuzzy based maximum power point tracking control along with harmonic elimination. Int. Trans on Electrical Energy Systems. 2020; DOI 10.1002/ett.3856.

8. S. K. Singh, P. A. Vardhan, P. Anand, S. N. Singh. A Novel Fuzzy Logic Solar (PV) - Grid / DG Powered Pump Controller for Efficient Water Management. Int. Journal of Electronics and Electrical Engineering. 2012; ISSN 2277-7040 1(1):37-44.
9. Y. S. Cheng, Y. H. Liu, H. C. Hesse, M. Naumann, C. N. Truong, A. Jossen. A PSO-optimized fuzzy logic control-based charging method for individual household battery storage systems within a community. Energies. 2018;11(2).
10. R. Al Badwawi, W. Issa, T. Mallick, M. Abusara. DC microgrid power coordination based on fuzzy logic control. 18th European Conference on Power Electronics and Applications, EPE 2016 ECCE. 2016:1-10.
11. S. Zenned, H. Chaouali, A. Mami. Fuzzy Logic Energy Management Strategy of a Hybrid Renewable Energy System Feeding a Typical Tunisian House. Int. Journal of Advanced Computer Science and Applications. 2017;8(12):206–212.
12. Kwi-Seong Jeong, Won-Yong Lee, Chang-Soo Kim. Energy management strategies of a fuel cell/battery hybrid system using fuzzy logics. Journal of Power Sources. 2005:1-8.
13. Amin Hajizadeh, Masoud Aliakbar Golkar. Intelligent power management strategy of hybrid distributed generation system. Electrical Power and Energy Systems. 2007:1-13.
14. Yu-Kai Chen, Member, IEEE, Yung-Chun Wu, Chau-Chung Song, Yu-Syun Chen. Design and Implementation of Energy Management System with Fuzzy Control for DC Microgrid Systems. IEEE Transactions on Power Electronics. 2013;28(4).
15. Anil Annamraju, Srikanth Nandiraju. Robust Frequency Control in an Autonomous Microgrid: A Two-Stage Adaptive Fuzzy Approach. Electric Power Components and Systems. 2018;46(1).
16. Marcelo Godoy Simões, Abdullah Bubshait. Frequency Support of Smart Grid Using Fuzzy Logic-Based Controller for Wind Energy Systems. Energies. 2019.
17. Abdelouahed Selmani, Mohamed Outanoute, Hassan Oubehar, Abdelali Ed-Dahhak, Abdeslam Lachhab, Mohammed Guerbaoui, Benachir Bouchikhi. An Embedded Solar-Powered Irrigation System Based on a Cascaded Fuzzy Logic Controller. Int. Trans on Electrical Energy Systems. 2019; DOI 10.1002/asjc.2220.
18. Shahid Hussain, Mohamed A. Ahmed, Young-chon Kim. Efficient Power Management Algorithm Based on Fuzzy Logic Inference for Electric Vehicles Parking Lot. IEEE Access. May 2019.

19. Y. Yuan, T. Zhang, B. Shen, X. Yan, T. Long. A fuzzy logic energy management strategy for a photovoltaic/diesel/battery hybrid ship based on experimental database. Energies. August 2018; 11(9).
20. Mehdi Hosseinzadeh, Farzad Rajaei Salmasi. Power management of an isolated hybrid AC/DC micro-grid with fuzzy control of battery banks. IET Renewable Power Generation. 2015; DOI 10.1049/iet-rpg.2014.0271.
21. Chendi Li, Yuanrui Chen, Dongbao Zhou, Junfeng Liu, Jun Zeng. A High-Performance Adaptive Incremental Conductance MPPT Algorithm for Photovoltaic Systems. Energies. 2016; DOI 10.3390/en9040288.
22. Mazen Abdel-Salam, Mohamed-Tharwat El-Mohandes, Mohamed Goda. An improved perturb-and-observe based MPPT method for PV systems under varying irradiation levels. Solar Energy. 2018; DOI 10.1016/j.solener.2018.06.080.
23. B. Hauke. Basic Calculation of a Boost Converter's Power Stage. Texas Instruments Application Report SLVA372C–November 2009–Revised January 2014. 2014:1-9.
24. T. Thirumalkumar, D. S. Rani, B. Ramu, P. Harika. Fuzzy Logic Based Controller Effective Energy Management of Composite Energy Storage System Involving Battery and Ultracapacitor in Microgrid. Journal of Electrical and Electronics Engineering. 2013;6(4) e-ISSN: 2278-1676, p-ISSN: 2320-3331:11-20.
25. H. Karshenas, H. Daneshpajooh. Bidirectional DC-DC Converters for Energy Storage Systems. Energy Storage Emerg. ERA Smart Grids. 2011:162-178.
26. IEEE 1547-2018. IEEE Standard for Interconnection and Interoperability of Distributed Energy Resources with Associated Electric Power Systems Interfaces Sponsored by the IEEE Standard for Interconnection and Interoperability of Distributed Energy Resources with Associate. 2018.
27. Texas Instruments, TI Designs: TIDA-01168. Bidirectional DC-DC Converter Reference Design for 12-V/48-V Automotive Systems. Documentation Report TIDUCS2B–June 2017–Revised March 2018:1-80.
28. H. Julian. Basic Calculations of a 4 Switch Buck-Boost Power Stage. Texas Instruments Application Report SLVA535B–January 2018–Revised July 2018.
29. M. Aneke, M. Wang. Energy storage technologies and real-life applications – A state of the art review. Appl. Energy. 2016; 179:350-377.
30. S. Koohi-Fayegh, M.A. Rosen. A review of energy storage types, applications and recent developments. Journal of Energy Storage. 2020; 27:101047.

Table 1: Energy Requirement of Critical Loads

S/N	Load	Quantity	Power (W)	Hour (hr)
1.	Light bulb	4	20	11
2.	Dishwasher	1	65	8
3.	LED TV	1	60	7
4	Laptops	2	60	6
5.	Gadgets	4	19	9

Table 2: Parameters of PV Module at STC

Parameter	*Value*
Maximum Power	249.5 W
Open Circuit Voltage (V_{OC})	23.11 V
Maximum Power Point Voltage (V_{max})	21.63 V
Short Circuit Current (I_{SC})	12.0 A
Maximum Power Point Current (I_{max})	11.53 A
Module Efficiency	15.26%
Characteristic Impedance (R_{CH})	1.876 Ω
Fill Factor	0.8997

Table 3: Fuzzy Logic Rule

1. If SOC is below 20% then dc/dc converter is at 1
2. If SOC is below 20% OR Load is at the LV-bus then dc/dc converter is at 1

3. If SOC is below 20% AND Load is at the LV-bus then dc/dc converter is at 1
4. If SOC is between 20% and 99% AND Load is at the LV-bus then dc/dc converter is at 1
5. If SOC is between 20% and 99% OR Load is at the HV-bus then dc/dc converter is at 1
6. If SOC is between 20% and 99% AND Load at bus AND off-grid, dc/dc converter is at 0
† At Decisions: “1” = Battery charges; “0” = Battery discharges. Rule 1 and Rule 6 are default.

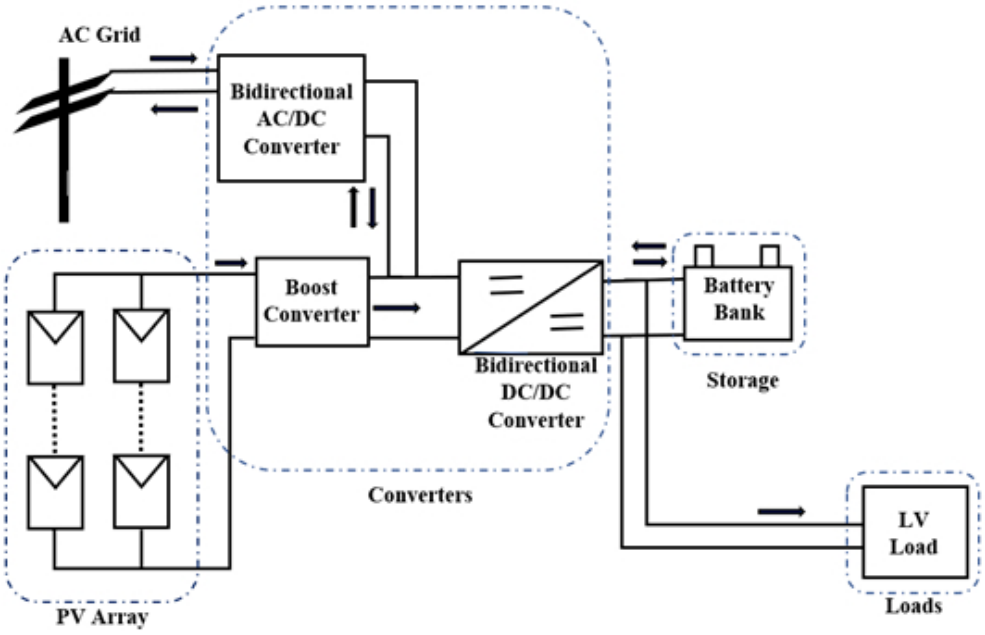

Fig. 1: Block Diagram of System Design

142x90mm (96 x 96 DPI)

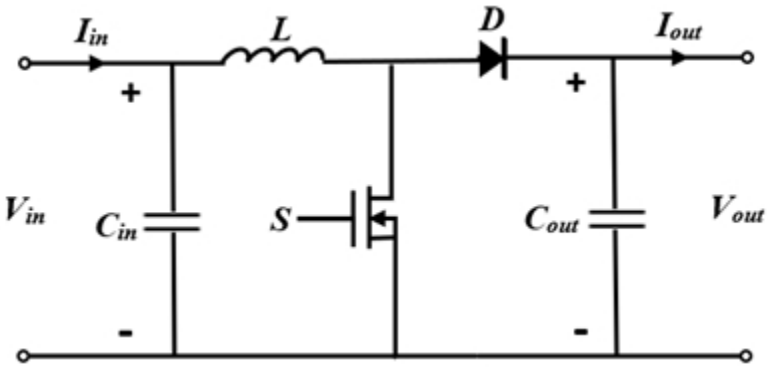

Fig. 2: Configuration of the Boost Converter

102x47mm (96 x 96 DPI)

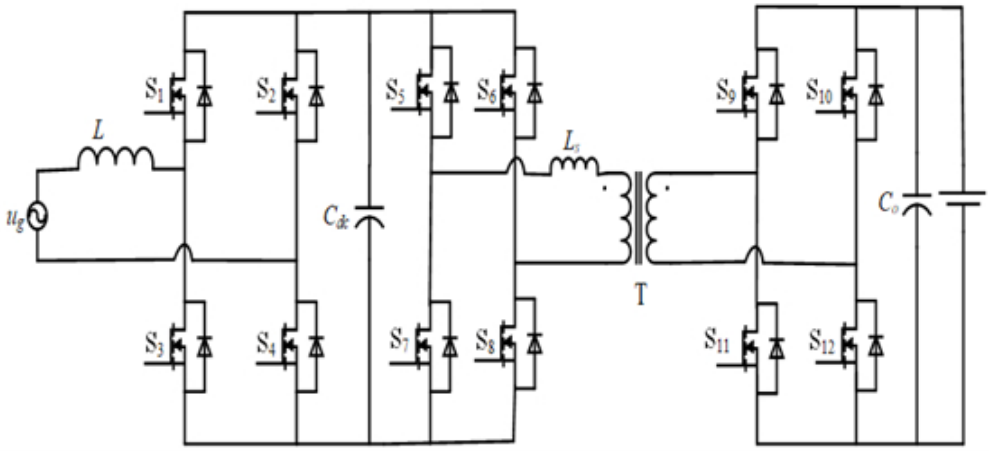

Fig. 3: Topology of AC-DC Converter with DAB

146x66mm (96 x 96 DPI)

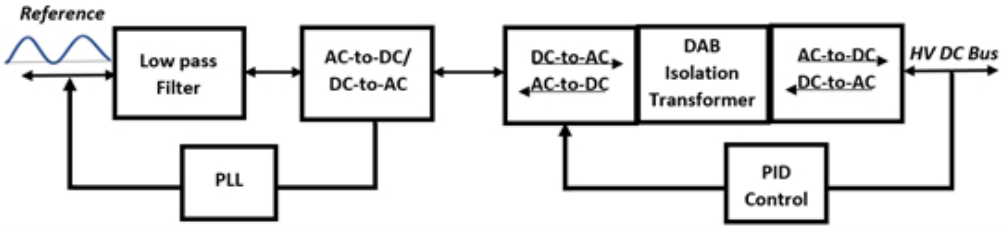

Fig. 4: Single-phase Bidirectional AC-DC Converter Block

142x32mm (96 x 96 DPI)

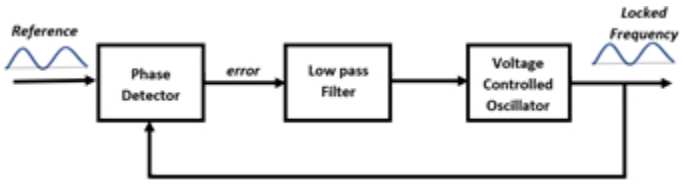

Fig. 5: Frequency Control – Phase Lock Loop (PLL) Block

89x23mm (96 x 96 DPI)

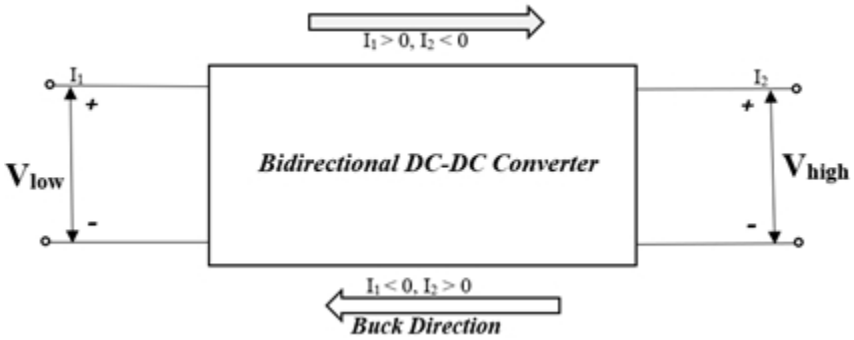

Fig. 6: Operation of Bidirectional DC-DC Converter

112x45mm (96 x 96 DPI)

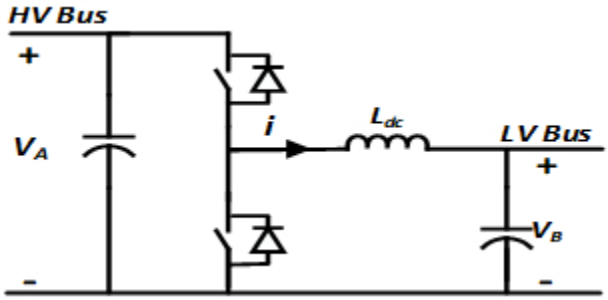

Fig. 7: Basic Bidirectional DC-DC Converter

83x40mm (96 x 96 DPI)

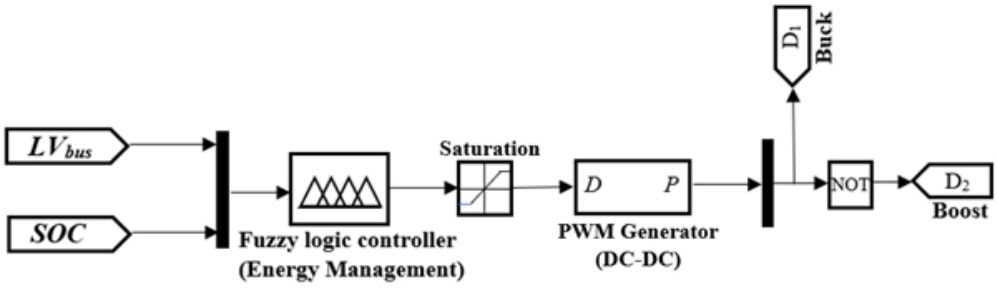

Fig. 8: Fuzzy Logic Control Block of Bidirectional DC-DC Converter

159x44mm (96 x 96 DPI)

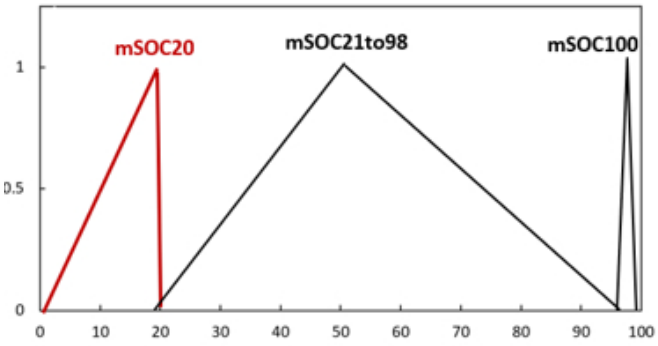

(a) *SOC* Function

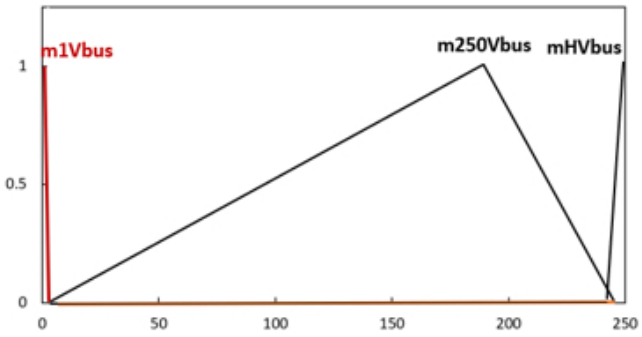

(b) *LVLoad* Function

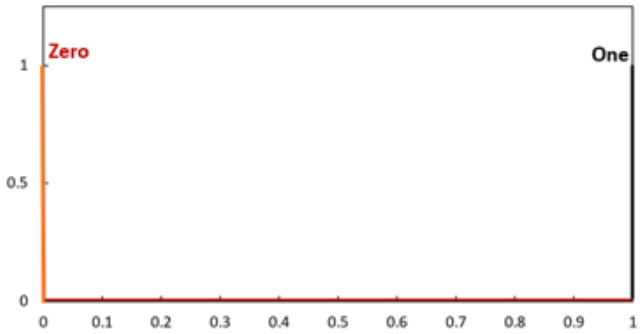

(c) *Decision* Function

Fig. 9: SOC, LVLoad, and Decision Membership Functions

98x180mm (96 x 96 DPI)

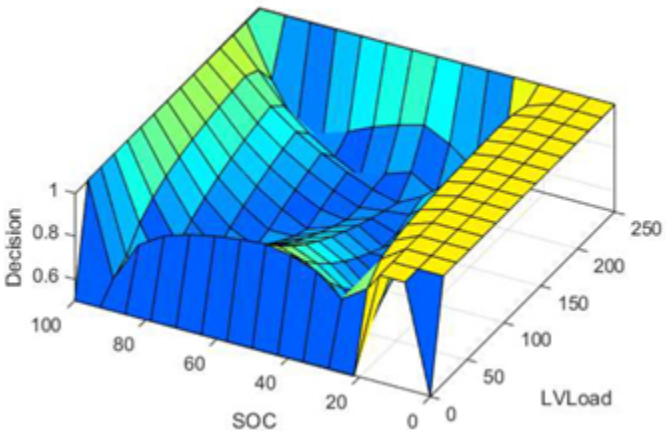

Fig. 10: Logic Surface Viewer

87x57mm (96 x 96 DPI)

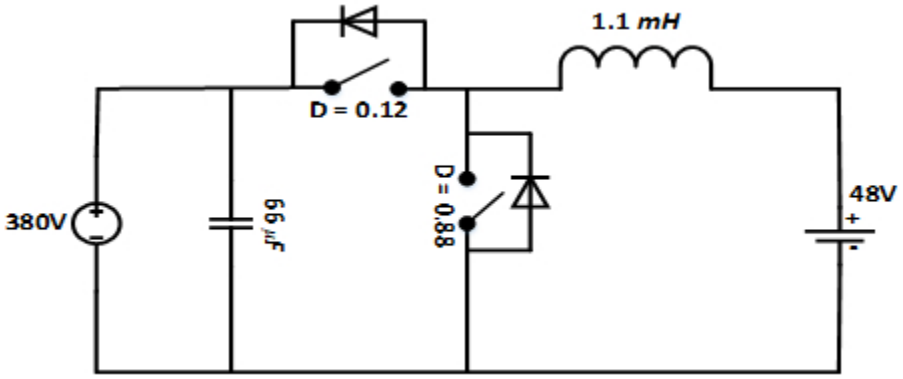

Fig. 11: Designed Bidirectional DC-DC Converter

119x51mm (96 x 96 DPI)

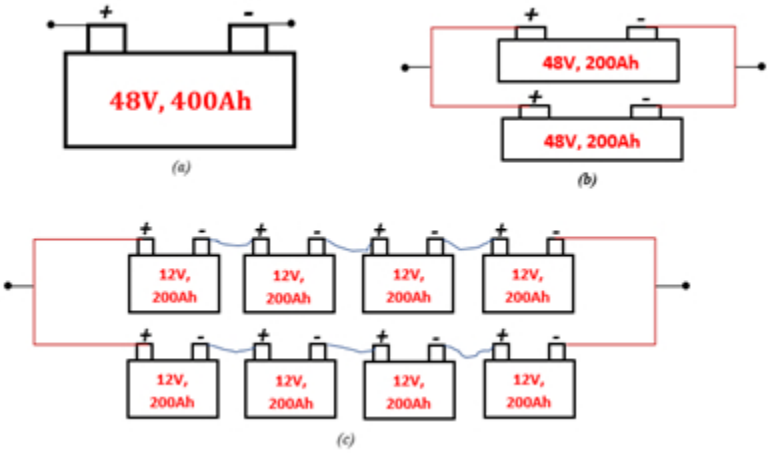

Fig. 12: (a) Single 48V 400Ah Rated Battery (b) Two 48V 200Ah Battery Units in Parallel (c) Eight 12V 200Ah Battery Units

102x60mm (96 x 96 DPI)

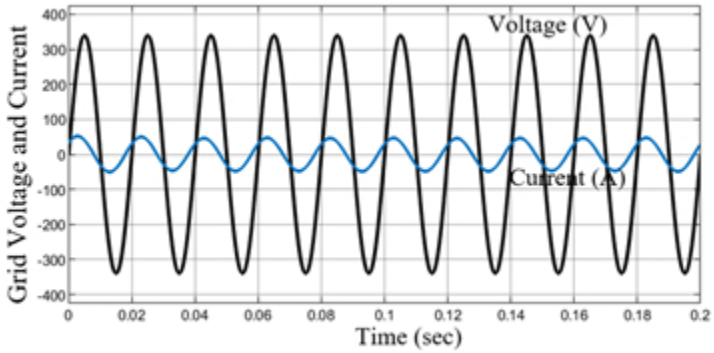

Fig. 13: Grid Voltage and Current

96x48mm (96 x 96 DPI)

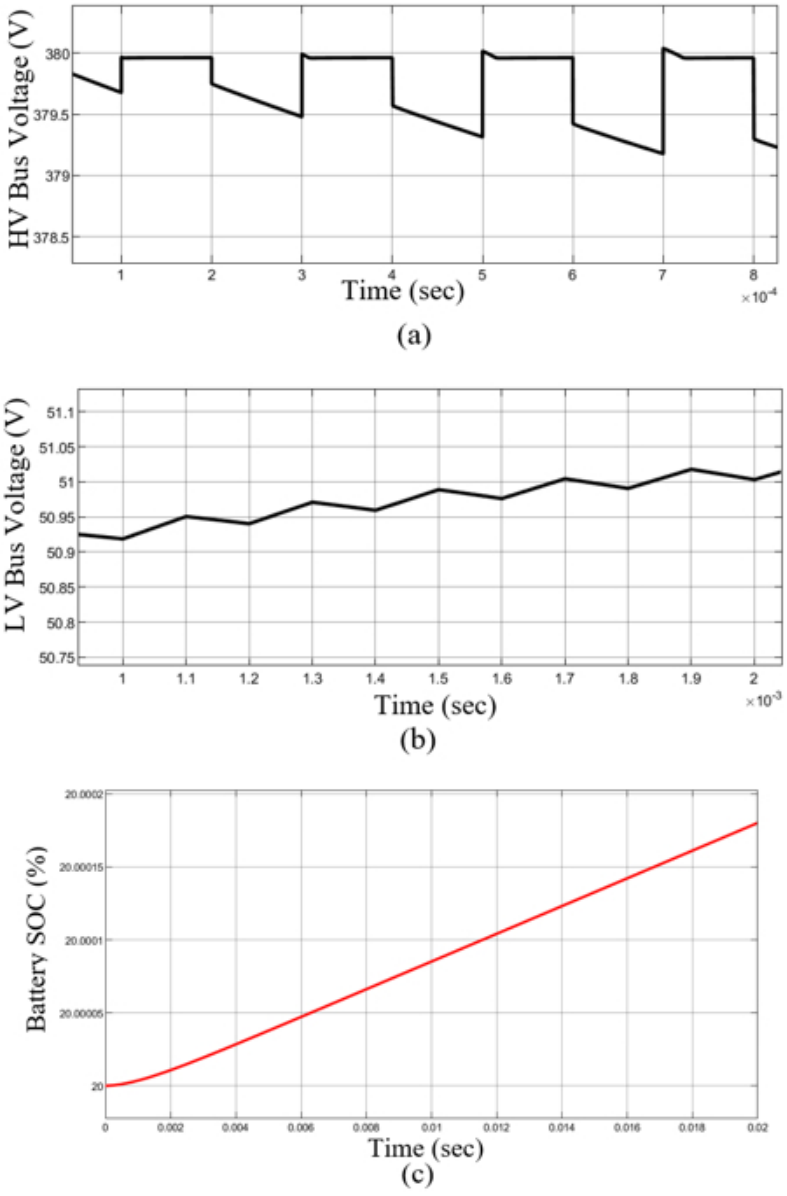

Fig. 14: (a) HV-bus Voltage (b) LV-bus Voltage (c) Battery SOC at STC

119x181mm (96 x 96 DPI)

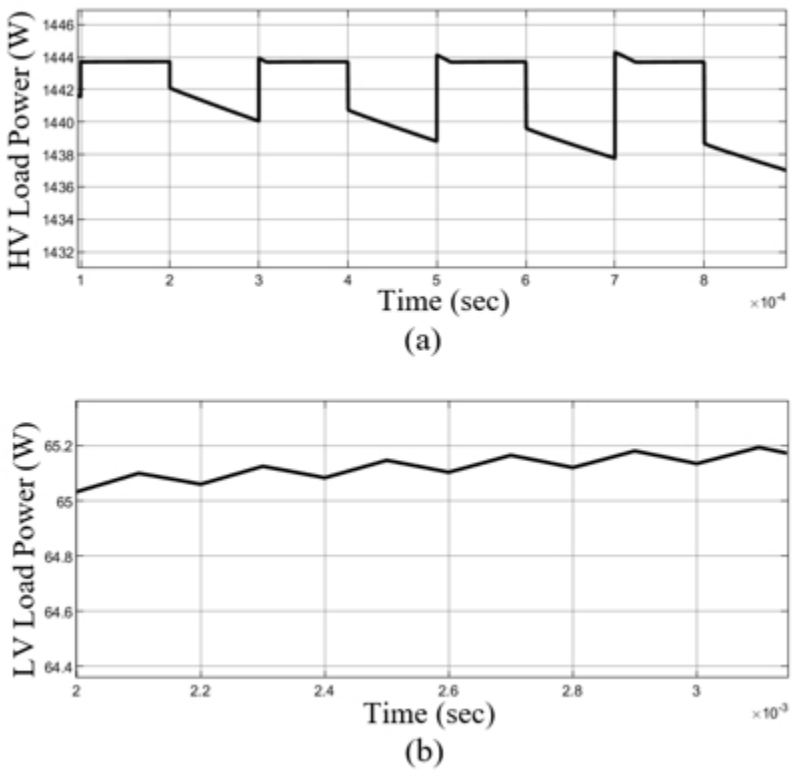

Fig. 15: (a) HV-bus Load Power (b)LV-bus Load Power

106x102mm (96 x 96 DPI)

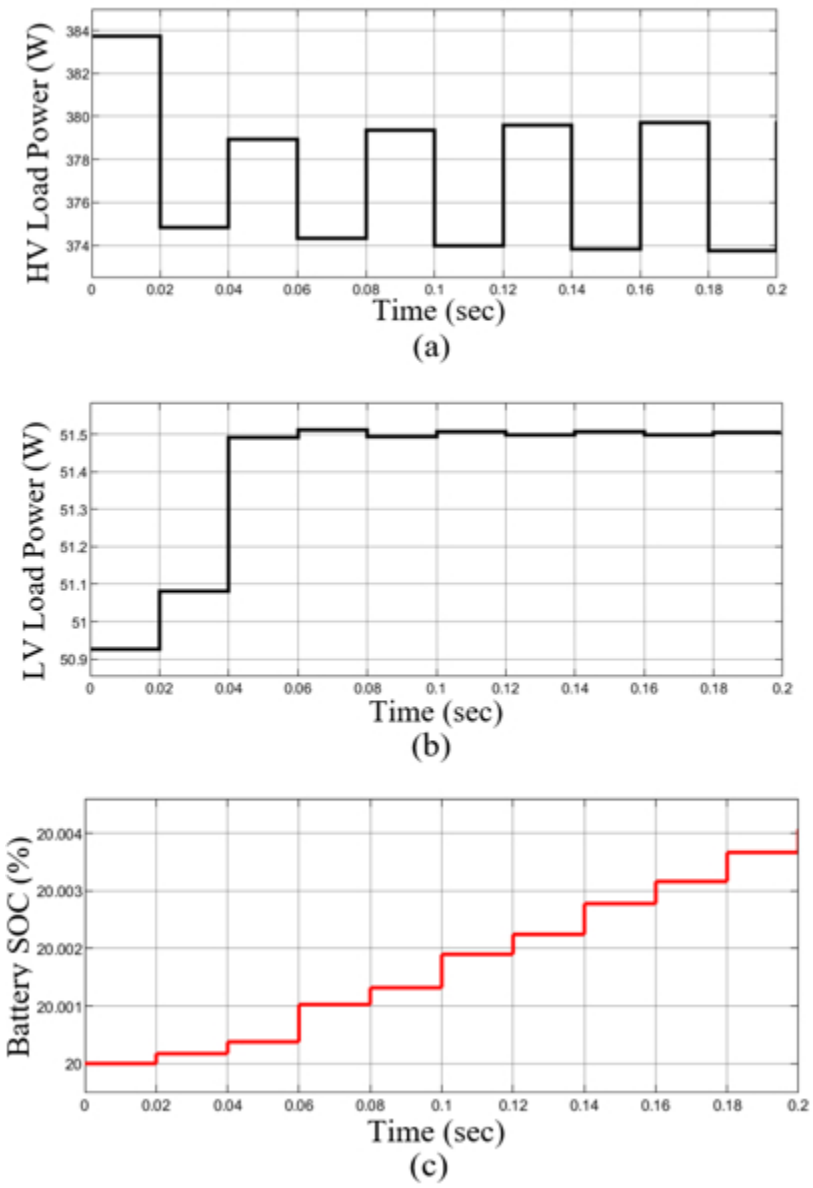

Fig. 16: (a) HV-bus Load Power (b) LV-bus Load Power (c) Battery SOC

107x156mm (96 x 96 DPI)

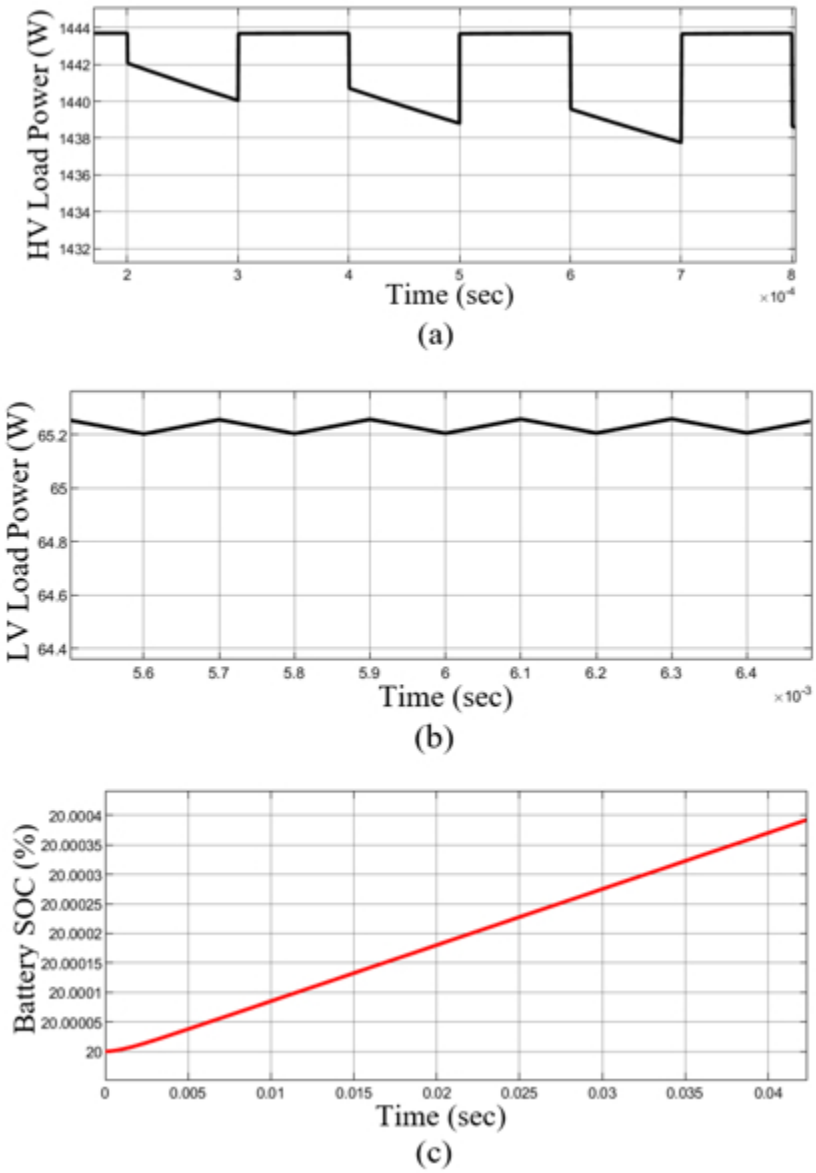

Fig. 17: (a) HV-bus Load Power (b) LV-bus Load Power (c) Battery SOC

110x155mm (96 x 96 DPI)

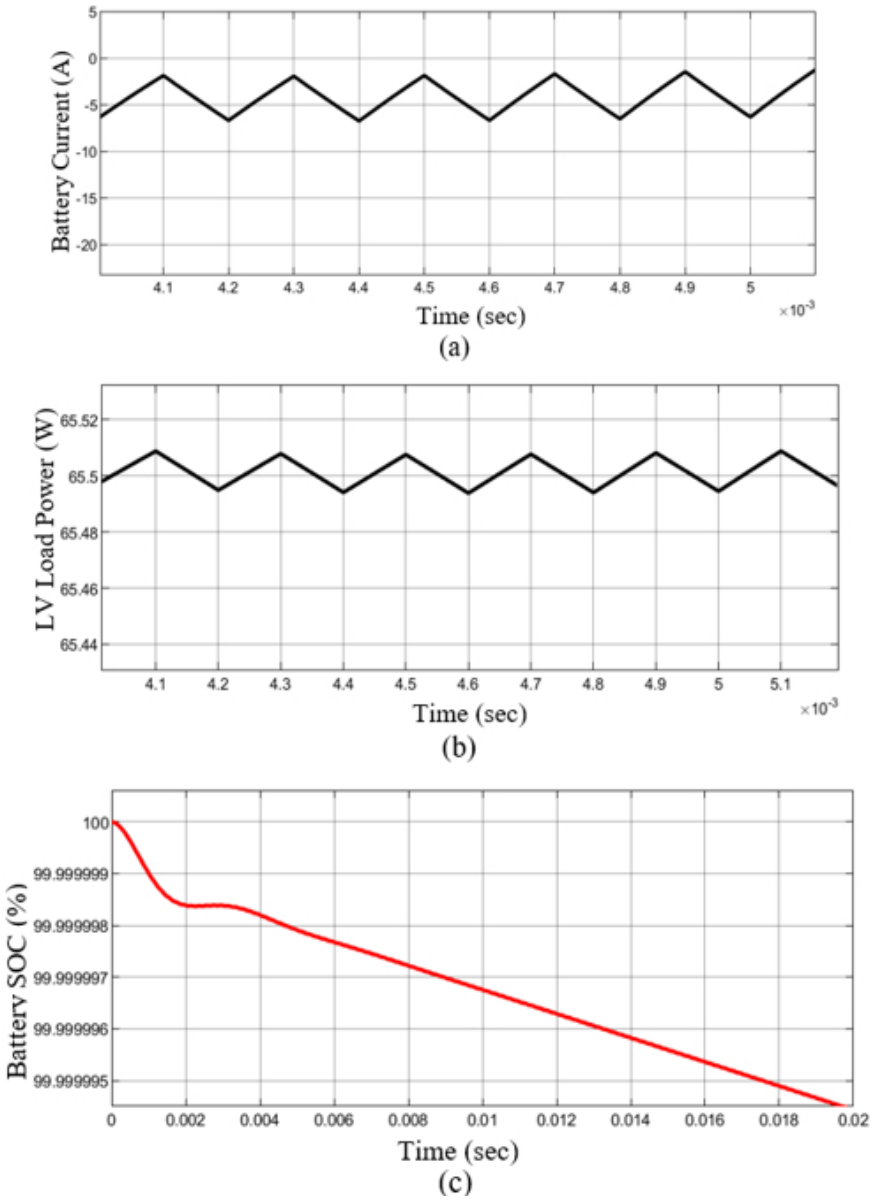

Fig. 18: (a) Battery Current (b) LV-bus Load Power (c) Battery SOC

136x179mm (96 x 96 DPI)